Proc. Natl. Acad. Sci. USA
Vol. 95, pp. 6728–6732, June 1998
Biochemistry

Two-domain reconstitution of a functional protein histidine kinase

HEIYOUNG PARK, SOUMITRA K. SAHA, AND MASAYORI INOUYE*

Department of Biochemistry, University of Medicine and Dentistry of New Jersey-Robert Wood Johnson Medical School, 675 Hoes Lane, Piscataway, NJ 08854-5635

Edited by Sung-Hou Kim, University of California, Berkeley, CA, and approved March 23, 1998 (received for review December 22, 1997)

ABSTRACT **In prokaryotes, in the absence of protein serine/threonine/tyrosine kinases, protein histidine kinases play a major role in signal transduction involved in cellular adaptation to various environmental changes and stresses. Histidine kinases phosphorylate their cognate response regulators at a specific aspartic acid residue with ATP in response to particular environmental signals. In this His-Asp phosphorelay signal transduction system, it is still unknown how the histidine kinase exerts its enzymatic function. Here we demonstrate that the cytoplasmic kinase domain of EnvZ, a transmembrane osmosensor of *Escherichia coli* can be further divided into two distinct functional subdomains: subdomain A [EnvZ(C)·(223–289); 67 residues] and subdomain B [EnvZ(C)·(290–450); 161 residues]. Subdomain A, with a high helical content, contains the autophosphorylation site, H–243, and forms a stable dimer having the recognition site for OmpR, the cognate response regulator of EnvZ. Subdomain B, an α/β-protein, exists as a monomer. When mixed, the two subdomains reconstitute the kinase function to phosphorylate subdomain A at His-243 in the presence of ATP. Subsequently, the phosphorylated subdomain A is able to transfer its phosphate group to OmpR. The two-domain structure of this histidine kinase provides an insight into the structural arrangement of the enzyme and its transphosphorylation mechanism.**

In prokaryotes the histidyl-aspartyl (His-Asp) phosphorelay signal transduction system plays a major role in cellular adaptation to various environmental stresses and growth conditions, and indeed *Escherichia coli* contains a large number of protein histidine kinases involved in the signal transduction (1–5). The transmembrane sensors involved in the His-Asp phosphorelay signal transduction usually contain the histidine kinase activity in their cytoplasmic signaling domain, except for those involved in chemotaxis. The histidine-kinase sensors are known to function as a dimer, whereas Tar, a chemosensor for aspartate, may, be able to transduce a signal within a single cytoplasmic domain (6, 7). In the process of the signal transduction, autophosphorylation of sensor histidine kinases occurs first through a bimolecular transphosphorylation reaction. This was originally demonstrated by complementation experiments with two defective mutants of EnvZ, a transmembrane osmosensor of *E. coli* and Taz1, a hybrid sensor between Tar and EnvZ (8, 9). In the case of Taz1, asymmetric binding of its ligand, aspartate, at the interphase of two Taz1 receptor domains in a dimer modulates the function of the cytoplasmic signaling domain in the dimer (10–12). The fact that autophosphorylation of histidine kinases, an obligatory step for phosphorylation of a downstream response regulator, occurs by a transphosphorylation reaction has also been shown with other histidine kinases (13–18).

EnvZ consists of the periplasmic putative receptor domain from residue 48 to 162, which is anchored in the cytoplasmic membrane with two transmembrane domains (TM1, residues 16–47; TM2, residues 163–179) (19). The second membrane segment connects to the cytoplasmic signaling domain from residue 180 to 450 and is responsible for the histidine kinase activity. This domain undergoes autophosphorylation at His-243 with ATP (20), and the phosphate group is subsequently transferred to Asp-55 of OmpR. OmpR is a response regulator for EnvZ and functions as a transcription factor for the outer membrane porin genes, *ompC* and *ompF* (21, 22). The EnvZ-signaling domain performs dual enzymatic functions, one as a kinase for OmpR and the other as a phosphatase for phosphorylated OmpR. The ratio of kinase and phosphatase activities is considered to control the level of phosphorylated OmpR (23–25). However, the exact regulatory mechanism by which EnvZ exerts its catalytic functions is still very poorly understood.

In the present report, we demonstrate that the cytoplasmic signaling domain of EnvZ can be further divided into two distinct subdomains, subdomain A (67 residues) and subdomain B (161 residues), to complement the kinase function by each other to phosphorylate the EnvZ cognate response regulator, OmpR. The two-domain structure of the histidine kinase provides a clue for its structural arrangement for the unique transphosphorylation reaction mechanism.

MATERIALS AND METHODS

Strains and Plasmids. *E. coli* B BL21-DE3 (F^- *ompT* r_B^- m_B^-) was used for the expression and purification of wild-type and mutant EnvZ(C) proteins (25). Construction of plasmid pET11a-EnvZ(C) was described elsewhere (25). pET11a-EnvZ(C)·ΔL, which contains the EnvZ sequence encoding residues Met-223 to Gly-450, was constructed by the digestion of pET11a-EnvZ(C) with *Nde*I followed by self-ligation. A linker,

```
5′-TATGCACCATCACCATCACCA-3′
   3′-ACGTGGTAGTGGTAGTGGTAT-5′,
```

was inserted at the *Nde*I site of pET11a-EnvZ(C)·ΔL, generating pPH006, which encodes H6-EnvZ(C)·ΔL. The construct was confirmed by DNA sequencing (Sequenase, United States Biochemical). The 1.4-kb *Xba*I–*Eco*RI fragment from pPH006 was used for site-directed mutagenesis (*in vitro* mutagenesis system, Sculptor, Amersham) to create a stop codon at either Thr-397 or Thr-290. For this purpose, 5′-AGTGCGCGCT-GAATTAGCGG-3′ and 5′-TACCTGCGCTAAGGGCAG-GAG-3′ oligomers were used, respectively. After the mutations were confirmed by DNA sequencing, the 1.4-kb X*ba*I–*Eco*RI fragments containing the mutations were subcloned

The publication costs of this article were defrayed in part by page charge payment. This article must therefore be hereby marked "*advertisement*" in accordance with 18 U.S.C. §1734 solely to indicate this fact.

This paper was submitted directly (Track II) to the *Proceedings* office.
Abbreviations: TM1 and TM2, transmembrane domains 1 and 2, respectively; NTA, nitrilotriacetic acid.
*To whom reprint requests should be addressed. e-mail: inouye@rwja.umdnj.edu.

back into pPH006. Thus, the plasmid designated pPH007 for Thr-398 (ACC) → (TGA) encodes H6-EnvZ(C)·ΔG2, and pPH009 for Thr-290 (ACC) → (TAA) encodes H6-EnvZ(C)·(223–289), respectively. pET11a-EnvZ(C)·(223–289) was obtained by digestion of pPH009 with *Nde*I, followed by self-ligation. For the construction of plasmid pET11a-Env(C)·(290–450) containing the EnvZ sequence from Thr-290 to Gly-450, PCR was carried out with primer 7109 (5′-CGCATATGACCGGGCAGGAG-3′), which contained an *Nde*I site to substitute Arg-289 (CGC) with Met (ATG), and primer 4163 (5′-TCGGATCCCGTTTATTTAC-3′), which contained a *Bam*HI site downstream of the Gly-450 codon. pET11a-EnvZ(C)·ΔL was used as the template. The 507-bp PCR fragment thus obtained was digested with *Nde*I and *Bam*HI and subcloned into the pET11a-EnvZ(C)·ΔL vector cut with *Nde*I and *Bam*HI. The sequence of the PCR product was confirmed by DNA sequencing as described (25).

Biochemical Assays of EnvZ and EnvZ(C) Constructs. Autophosphorylation, phosphotransfer to OmpR, and phospho-OmpR phosphatase activity were determined essentially as described (8, 25). The phosphorylated OmpR was prepared as follows. The membrane fraction containing EnvZ-T247R (kinase$^+$/phosphatase$^-$) was first phosphorylated with 50 μCi of [γ-^{32}P]ATP (1.67 nmol) in 200 μl of buffer A [50 mM Tris·HCl (pH 8.0)/50 mM KCl/5 mM $CaCl_2$/1 mM phenylmethylsulfonyl fluoride/5% glycerol], for 20 min at room temperature. The reaction mixture was centrifuged at 393,000 × *g* for 14 min at 4°C by using a Beckman TL-100 ultracentrifuge. The membrane pellet was washed five times with 200 μl of buffer A, sonicated, and then resuspended in the same buffer. Purified OmpR protein was incubated with the membrane fraction containing phosphorylated EnvZ-T247R for 20 min at room temperature to allow phosphotransfer to OmpR. After incubation, the reaction mixture was centrifuged at 393,000 × *g* for 14 min at 4°C to remove the membrane containing EnvZ-T247R. The supernatant containing phospho-OmpR was then applied to a G-50 gel filtration column (0.6 × 7 cm; Pharmacia) to remove residual [γ-^{32}P]ATP and inorganic phosphate ($^{32}P_i$). Each fraction was analyzed by TLC to confirm that the phospho-OmpR preparation was not contaminated with [γ-^{32}P]ATP or $^{32}P_i$. The fractions containing only phospho-OmpR were pooled and total OmpR protein concentration was measured by a Bio-Rad protein concentration assay. During preparation, protein solutions were kept on ice.

Binding Assay on Ni-Nitrilotriacetic Acid (NTA) Resin. Purified proteins, EnvZ(C)·(223–289) plus either H6-EnvZ(C)·wt or H6-EnvZ(C)·(223–289), were mixed in 20 μl of buffer I [50 mM sodium phosphate buffer (pH 7.8)/0.3 M NaCl/5% glycerol] at room temperature for 30 min, 10 μl of Ni-NTA resin (50%, vol/vol) was added to the protein mixture, and the sample was incubated for 30 min on ice. After the sample was washed three times with buffer II [50 mM sodium phosphate buffer (pH 6.0)/0.3 M NaCl/5% glycerol] by using ultrafree-MC centrifugal filters (Millipore), proteins bound to Ni-NTA resin were eluted with 0.2 M imidazole/buffer II. The binding experiments between OmpR and either H6-EnvZ(C)·wt or H6-EnvZ(C)·(223–289) were carried out as described (26). The proteins eluted with 0.2 M imidazole/buffer II in each binding assay were subjected to SDS/PAGE (20% gel) and then stained with silver (27).

CD Spectral Analysis. The CD spectrum was obtained by using an Aviv model 62DS spectrophotometer at 25°C. Far-UV CD spectra (200–250 nm) of EnvZ(C)·(223–289) and EnvZ(C)·(290–450) in sodium phosphate buffer [50 mM sodium phosphate (pH 7.4)/0.3 M KCl/1 mM phenylmethylsulfonyl fluoride] were measured in a cuvette with a 1-cm path length. Protein concentrations of EnvZ(C)·(223–289) and EnvZ(C)·(290–450) were 0.338 and 0.118 mg/ml, respectively. These values were determined by A_{280} and calculated based on protein molar extinction coefficients, which are 2,680 for EnvZ(C)·(223–289) and 20,910 for EnvZ(C)·(290–450) (28).

Analytical Size Exclusion Chromatography and Light Scattering. Gel filtration chromatography of the purified EnvZ(C)·(223–289) or EnvZ(C)·(290–450) protein was accomplished by using a TSK-GEL column (Tosohaas, Montgomeryville, PA) equipped with an HPLC system (model 110B, Beckman). Protein samples and standard marker proteins were loaded in an equal volume (0.2 ml) to the column preequilibrated with buffer [20 mM Tris·HCl (pH 8.0)/350 mM ammonium acetate/200 mM NaCl/2 mM DTT/10% glycerol/100 mM sodium azide/1 mM phenylmethylsulfonyl fluoride] at a flow rate of 0.5 ml/min. The A_{280} of the fractions was monitored, and fractions at each peak were pooled. The V_o of the column was determined by using blue dextran 2000. For the light-scattering experiment, EnvZ(C)·(223–289) (6.5 mg/1iter) and EnvZ(C)·(290–450) (4.5 mg/1iter) proteins were analyzed with a DanaPro-801

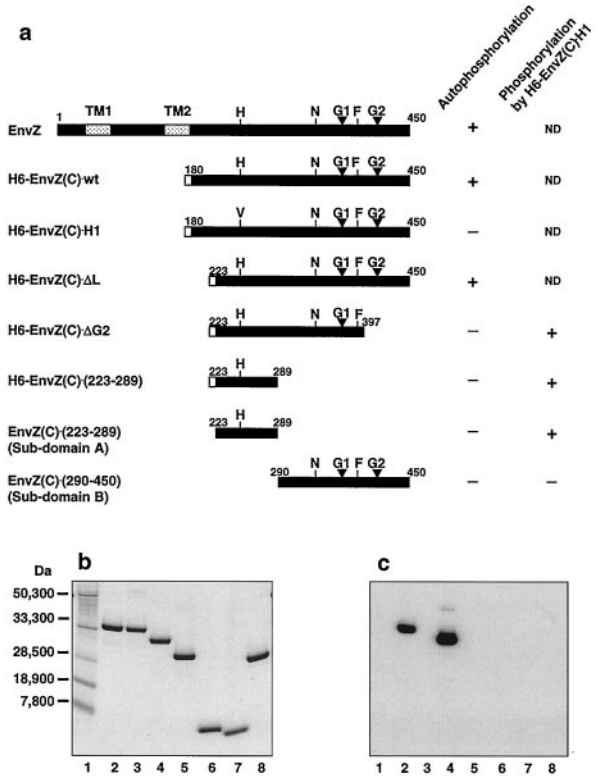

FIG. 1. Purification and autophosphorylation of various EnvZ(C) fragments. (*a*) Serial deletions of EnvZ(C) proteins. The N- and C-terminal amino acid residue numbers of each EnvZ(C) fragment are shown above ends of the bar. Solid bars represent the EnvZ sequence. TM1 and TM2 are indicated by shaded boxes. The open bars at the left side of the bars indicate the six histidine residues [Met-(His)6] at the N-terminal end. Conserved motifs among all of the histidine kinases, H243, N347, F387, and two glycine-rich regions, G1 (residues 373–377) and G2 (residues 403–405), are shown on the top of the full-length EnvZ. The activities of autophosphorylation and phosphorylation by EnvZ(C)·H1 of each protein are indicated by + or − (no activity) or ND (not determined). (*b* and *c*) Purified EnvZ(C) fragments (3 μg each) were incubated with 0.2 μCi (6.7 pmol) of [γ-^{32}P]ATP in a 20-μl reaction mixture consisting of 50 mM Tris·HCl (pH 8.0), 50 mM KCl, 5 mM $CaCl_2$, 5% glycerol, and 1 mM phenylmethylsulfonyl fluoride (buffer A) for 10 min at room temperature, and the autophosphorylation reaction was stopped by adding 5× SDS gel loading buffer. The reaction mixture was subjected to SDS/PAGE with a 16% Tricine gel (NOVEX, San Diego), followed by Coomassie brilliant blue staining (*b*) and autoradiography (*c*). Lanes: 1, protein molecular mass markers; 2, H6-EnvZ(C)·wt; 3, H6-EnvZ(C)·H1; 4, H6-EnvZ(C)·ΔL; 5, H6-EnvZ(C)·ΔG2; 6, H6-EnvZ(C)·(223–289); 7, EnvZ(C)·(223–289); 8, EnvZ(C)·(290–450).

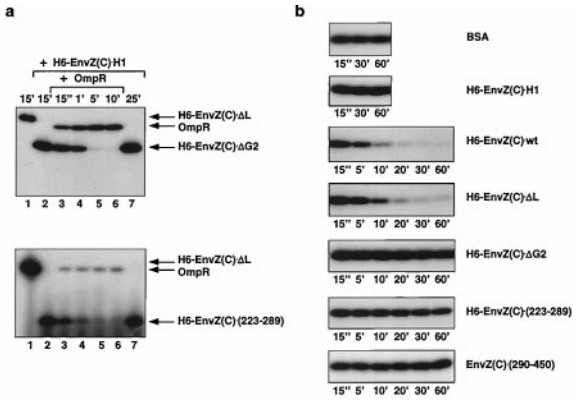

FIG. 2. Enzymatic assay of various EnvZ(C) fragments. (*a*) Kinase assay of EnvZ(C) fragments. The purified protein H6-EnvZ(C)·ΔL [0.13 μM in the upper panel with H6-EnvZ(C)·ΔG2 or 0.26 μM in the lower panel with H6-EnvZ(C)·(223–289)] was autophosphorylated with 0.2 μCi of [γ-^{32}P]ATP (6.7 pmol) at room temperature for 15 min as a control (lane 1). For *trans*-autophosphorylation of H6-EnvZ(C)·ΔG2 [or H6-EnvZ(C)·(223–289)] by H6-EnvZ(C)·H1, equimolar concentrations of each protein (1.3 μM each) were mixed and incubated with 0.2 μCi of [γ-^{32}P]ATP for 15 min (lane 2) and 25 min (lane 7) at room temperature. For the phosphotransfer reaction to OmpR, H6-EnvZ(C)·ΔG2 [or H6-EnvZ(C)·(223–289)] and H6-EnvZ(C)·H1 were mixed, and the mixture was first incubated for 15 min (lane 2). After incubation, OmpR was added to the mixture. The molar ratio of H6-EnvZ(C)·ΔG2 [or H6-EnvZ(C)·(223–289)] to H6-EnvZ(C)·H1 and OmpR was 1:1:1 (1.3 μM each). The phosphotransfer reaction was stopped by adding 5× SDS gel loading buffer at 15 s (lane 3), 1 min (lane 4), 5 min (lane 5), and 10 min (lane 6). The samples were then subjected to SDS/PAGE analysis followed by autoradiography. The position of each protein is indicated by an arrow. (*b*) Phosphatase assay of EnvZ(C) fragments. The phosphorylated OmpR in 2.6 μM of total OmpR protein (14) was incubated at room temperature with the following proteins: 2.6 μM of BSA, H6-EnvZ(C)·H1, H6-EnvZ(C)·wt, H6-EnvZ(C)·ΔL, H6-EnvZ(C)·ΔG2, H6-EnvZ(C)·(223–289), and EnvZ(C)·(290–450) as indicated at the right. The reaction was carried out in the presence of 1 mM ADP. The reaction times are indicated at the bottom of the figures. The reaction was stopped by adding 5× SDS gel loading buffer and analyzed by SDS/PAGE, followed by autoradiography.

dynamic light-scattering instrument (Protein Solution, Charlottesville, VA), and the molecular mass of each protein was determined by using the AutoPro software provided by the manufacture of the instrument. This work was kindly carried out in the laboratory of M. Ikura at the University of Toronto.

RESULTS

We first analyzed the kinase activity of the cytoplasmic domain of EnvZ (residue 180–450). It retained the activity even if it was detached from TM2 (Fig. 1*a*). We further shortened this domain by deleting the so-called linker region from residue 180 to 222, resulting in EnvZ(C)·ΔL (Fig. 1*a*), and still it retained both the kinase and phosphatase activities (Figs. 1*c*, lane 3, and 2*b*, respectively) (25). This 228-residue EnvZ fragment contains all of the features highly conserved in the histidine kinases (1–5), His-243 (autophosphorylation site), Asn-347, Phe-387, and the two Gly-rich boxes, G1 (DXGXG; 373–377) and G2 (GXG; 403–405) (Fig. 1*a*).

Next, to further dissect domain structures of H6-EnvZ(C)·ΔL, six histidine residues were tagged at the N-terminal end of EnvZ(C)·ΔL, the smallest kinase, we carried out limited tryptic digestion, and the mass spectrometer analysis of the tryptic fragments revealed that there are two major cleavage sites at Arg-289 and at Arg-397. Thus, two N-terminal fragments, one from residue 223 to 397 [H6-EnvZ(C)·ΔG2] and the other from residue 223 to 289 [H6-EnvZ(C)·(223–289) or EnvZ(C)·(223–289)] were generated (Fig. 1*a* and *b*). Note that Arg-397 is located between G1 and G2 boxes and H6-EnvZ(C)·ΔG2 was expressed mostly as inclusion bodies (not shown). From the functional assay, we found that not only H6-EnvZ(C)·ΔG2 but also H6-EnvZ(C)·(223–289), consisting of only 67 residues, were transphosphorylated by H6-EnvZ(C)·H1 (Fig. 2*a*, lanes 2 and 7). H6-EnvZ(C)·H1, in which autophosphorylation site His-243 is replaced with Val, is known to transphosphorylate EnvZ fragments deficient in kinase activity, even if it is unable to autophosphorylate itself (8, 9). Furthermore, these N-terminal fragments with H6-EnvZ(C)·H1 were able to phosphorylate OmpR (Fig. 2*a*, lanes 3–6), although they lost the phosphatase activity (Fig. 2*b*). It seems that the detachment of subdomains A and B abolishes the phosphatase activity, indicating that in contrast to the kinase activity the phosphatase activity is much more sensitive to the structural arrangement of the signaling domain. Our attempt to obtain a shorter fragment such as the fragment from Met-223 to Lys-272 was unsuccessful.

The above results suggest that EnvZ(C)·ΔL can be divided into two subdomains, A and B, at Arg-289: EnvZ(C)·(223–289) and EnvZ(C)·(290–450). Both subdomains were expressed as stable soluble proteins (Fig. 1*b*, lanes 7 and 8, respectively).

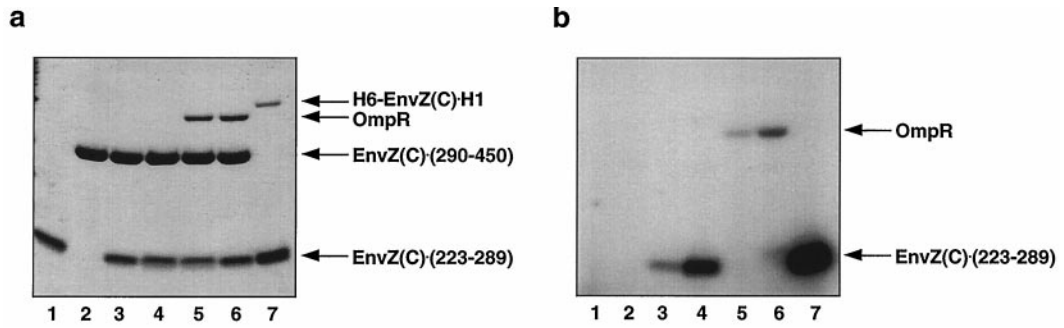

FIG. 3. The recovery of kinase activity by complementation between EnvZ(C)·(223–289) and EnvZ(C)·(290–450). EnvZ(C)·(223–289) (lane 1) or EnvZ(C)·(290–450) (lane 2) (1.2×10^{-5} M) was incubated with 0.5 μCi (17 pmol) of [γ-^{32}P]ATP for 20 min. For *trans*-autophosphorylation of EnvZ(C)·(223–289) (1.2×10^{-5} M) by EnvZ(C)·(290–450) (1.2×10^{-5} M), two proteins were incubated with 0.5 μCi of [γ-^{32}P]ATP (17 pmol) for 5 min (lane 3) and 20 min (lane 4). For the phosphotransfer reaction to OmpR, EnvZ(C)·(223–289) (1.2×10^{-5} M) was first *trans*-autophosphorylated by EnvZ(C)·(290–450) (1.2×10^{-5} M) with 0.5 μCi of [γ-^{32}P]ATP for 5 min (lane 3) and then OmpR (2.4×10^{-6} M) was added into the *trans*-autophosphorylation mixture, and the mixture was incubated for another 15 s (lane 5) and 15 min (lane 6). Lane 7 shows *trans*-autophosphorylation of EnvZ(C)·(223–289) (1.2×10^{-5} M) by H6-EnvZ(C)·H1 (2.4×10^{-6} M) with 0.5 μCi of [γ-^{32}P]ATP for 5 min. All reactions were conducted at room temperature in 20 μl of buffer A and stopped by adding 5× SDS gel loading buffer. Samples were then subjected to SDS/PAGE with a 16% Tricine gel (NOVEX), followed by staining with Coomassie brilliant blue (*a*) and autoradiography (*b*).

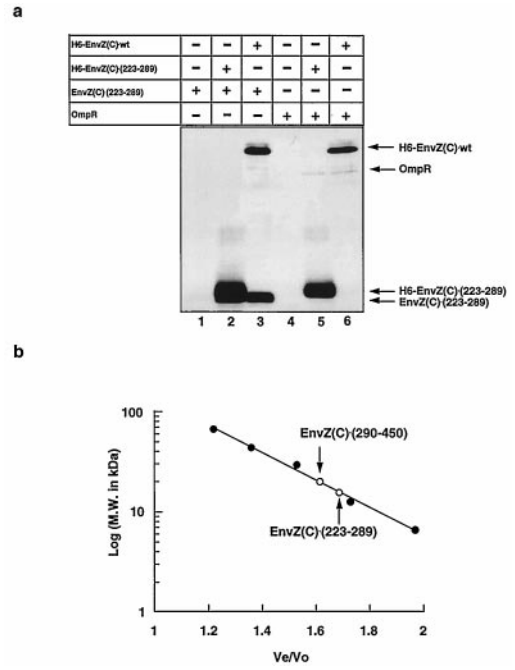

FIG. 4. Analysis of dimerization of EnvZ(C)·(223–289) and its interaction with OmpR. (*a*) The purified proteins were mixed at room temperature for 30 min (lanes 1–3) or 60 min (lanes 4–6) in 20 μl of buffer I [50 mM sodium phosphate (pH 8.0)/0.3 M NaCl/5% glycerol], 10 μl of Ni-NTA resin (50%, vol/vol; Qiagen, Chatsworth, CA) equilibrated with buffer I was added, followed by further incubation for 30 min on ice. After the sample was washed three times with buffer II [50 mM sodium phosphate (pH 6.0)/0.3 M NaCl/5% glycerol], proteins bound to Ni-NTA resin were eluted by 0.2 M imidazole in buffer II. Proteins thus eluted were subjected to SDS/PAGE (20% gel), and the gel was treated by silver staining. Lanes: 1, EnvZ(C)·(223–289) (2.5×10^{-5} M); 2, H6-EnvZ(C)·(223–289) and EnvZ(C)·(223–289) (2.5×10^{-5} M each); 3, H6-EnvZ(C)·wt and EnvZ(C)·(223–289) (2.5×10^{-5} M each); 4, OmpR (6.1×10^{-6} M); 5, OmpR (6.1×10^{-6} M) and H6-EnvZ(C)·(223–289) (2.5×10^{-5} M); 6, OmpR (6.1×10^{-6} M) and H6-EnvZ(C)·wt (2.5×10^{-5} M). (*b*) The gel filtration profiles of EnvZ(C)·(223–289) and EnvZ(C)·(290–450). The migrations of EnvZ(C)·(223–289) and EnvZ(C)·(290–450) were analyzed by using a TSK-GEL column (Tosohaas) equipped with an HPLC system (model 110B, Beckman). The standard proteins are indicated as closed circles; BSA (66,000 Da), ovalbumin (43,000 Da), carbonic anhydrase (29,000 Da), cytochrome *c* (12, 400 Da), and CspA (7, 400 Da). The proteins of EnvZ(C)·(223–289) and EnvZ(C)·(290–450) are indicated by open circles and arrows. The *y* axis represents the molecular mass (kDa) in a log scale; the *x* axis represents the ratio of the elution volume of sample (V_e) to the void volume (V_o).

Although subdomain B had neither autophosphorylation activity (Fig. 1*c*, lane 8) nor phosphatase activity (Fig. 2*b*), it was able to phosphorylate subdomain A when subdomains A and B were mixed in the presence of ATP (Fig. 3, lanes 3 and 4). In addition, when OmpR was added to the mixture, it was phosphorylated in a time-dependent manner (Fig. 3, lanes 5 and 6). If the transphosphorylation of subdomain A is compared with H6-EnvZ(C)·H1 (Fig. 3, lane 7), the phosphorylation efficiency with subdomain B was approximately 5%.

CD analysis of subdomain A showed a high α-helical content (55%), whereas subdomain B had both α-helix (29%) and β-sheet (26%; data not shown), suggesting that subdomain A is basically an αα-protein, and subdomain B is an αβ-protein. By using Ni-NTA resin (26), we found that subdomain A forms a dimer; it binds to resin only in the presence of His-tagged subdomain A [H6-EnvZ(C)·(223–289); compare lane 1 and lane 2 in Fig. 4*a*]. It also binds to H6-EnvZ(C)·wt (lane 3) as we expected from Fig. 2*a*. Because it has been demonstrated that EnvZ(C) forms a dimer (20, 26), the present result indicates that the region required for the dimer formation resides in the 67 residue of subdomain A. This domain also contains the region required for OmpR interaction, because OmpR was trapped on the resin only in the presence of His-tagged subdomain A (compare lane 4 and lane 5 in Fig. 4*a*). Note that the amount of OmpR bound to the resin in lane 5 is comparable to that with H6-EnvZ(C)·wt shown in lane 6. Consistent with this finding, when purified phosphorylated subdomain A was mixed with OmpR, the phosphoryl group was efficiently transferred to OmpR in the absence of subdomain B (data not shown).

We further explored the conformation of the existence of subdomain A as a dimer by size exclusion chromatography. The molecular mass of subdomain A was estimated to be 19.9 kDa by gel filtration (Fig. 4*b*). In addition, light-scattering data showed it to be 20 kDa, thereby fully consistent with our notion that subdomain A (calculated molecular mass, 7.6 kDa) forms a dimer. In contrast, the molecular mass of subdomain B (calculated molecular mass, 17.6 kDa) was 21.6 kDa by gel filtration (Fig. 4*b*) and 26.5 kDa by light scattering, indicating that this fragment exists as a monomer. These structural arrangements are now confirmed; the NMR solution structures of both subdomains were determined in collaboration with M. Ikura (Ontario Cancer Institute, Toronto).

DISCUSSION

Identification of the dimerization domain together with the fact that autophosphorylation occurs via transphosphorylation between two kinase molecules indicates that signal transduction by histidine kinases is carried out through bimolecular transphosphorylation reaction within a dimer. It is tempting to speculate that two EnvZ-signaling domains in a dimer symmetrically assemble in such a way as the phosphorylation domain (subdomain A) of one kinase interacts with the catalytic domain (subdomain B) of the other kinase to serve as a substrate for phosphorylation. Thus, unlike methyl-accepting chemotaxis receptors (6, 7), transmembrane signal transduction by histidine kinases cannot be carried out through a single cytoplasmic signaling domain, although the mechanisms for signaling across the membrane by methyl-accepting chemotaxis receptors and EnvZ have been shown to be similar (29, 30). It has been suggested that, when a hybrid receptor (Taz1) between Tar, a methyl-accepting chemotaxis receptors, and EnvZ is used, regardless of the ligand concentrations, the kinase activity is constant, whereas the phosphatase activity becomes inhibited as the ligand concentration increases (12). At high ligand concentrations signal transduction across the membrane may cause a change in the interaction between subdomains A and B to directly modulate the phosphatase activity or the binding of phospho-OmpR to the AB complex. At present, it is not known whether this interaction occurs intermolecularly, intramolecularly, or both ways. The phosphatase activity appears to be very sensitive to the structural arrangement of the signaling domain, because the phosphatase activity was undetectable in the complementation experiment with subdomains A and B in contrast to the kinase activity.

Our present work demonstrates that the histidine kinase EnvZ can be dissected into two smaller distinct domains: the 67-residue subdomain A as the phosphoreceptor dimerization domain, which also serves as the OmpR interaction domain, and the 161-residue subdomain B as the catalytic kinase domain. This structural arrangement provides us with means to study the structure and function of histidine kinases. Because both subdomains are highly soluble and their sizes are less than 20 kDa, the determination of their three-dimensional structures by NMR spectroscopy is now in progress. Because no crystals have been obtained for histidine kinases, the present system with complementary subdomains may be ideal for the structural determination of histidine kinases.

We thank Drs. S. L. Harlocker, U. Shinde, and K. Yamanaka and Ms. R. Dutta for critical reading of this manuscript and Dr. M. Ikura for providing the light-scattering data. We also thank Takara Shuzo Co. for mass spectrometer analysis of tryptic peptides. This work was supported by Grant GM 19043 from the National Institutes of Health.

1. Egger, L. A., Park, H. & Inouye, M. (1997) *Genes Cells* **2,** 167–184.
2. Appleby, J. L., Parkinson, J. S. & Bourret, B. R. (1996) *Cell* **86,** 845–848.
3. Inouye, M. (1996) *Cell* **85,** 13–14.
4. Parkinson, J. S. & Kofoid, E. C. (1992) *Annu. Rev. Genet.* **26,** 71–112.
5. Stock, J. B., Ninfa, A. J. & Stock, A. M. (1989) *Microbiol. Rev.* **53,** 450–490.
6. Gardina, P. J. & Manson, M. D. (1996) *Science* **274,** 425–426.
7. Tatsuno, I., Homma, N., Oosawa, K. & Kawagishi, J. (1996) *Science* **274,** 423–425.
8. Yang, Y. & Inouye, M. (1991) *Proc. Natl. Acad. Sci. USA* **88,** 11057–11061.
9. Yang, Y. & Inouye, M. (1993) *J. Mol. Biol.* **231,** 335–342.
10. Yang, Y., Park, H. & Inouye, M. (1993) *J. Mol. Biol.* **232,** 493–498.
11. Milburn, M. V., Prive, G. G., Milligan, D. L., Scott, W. G., Yen, J., Jancarik, J., Koshland, D. E., Jr., & Kim, S. H. (1991) *Science* **254,** 1342–1347.
12. Jin, T. & Inouye, M. (1993) *J. Mol. Biol.* **232,** 484–492.
13. Uhl, M. A. & Miller, J. F. (1996) *EMBO J.* **15,** 1028–1036.
14. Pan, S. Q., Charles, T., Jin, S., Wu, Z. L. & Nester, E. W. (1993) *Proc. Natl. Acad. Sci. USA* **90,** 9939–9943.
15. Ninfa, E. G., Atkinson, M. R., Kamberov, E. S. & Ninfa, A. J. (1993) *J. Bacteriol.* **175,** 7024–7032.
16. Swanson, R. V., Bourret, R. B. & Simon, M. I. (1993) *Mol. Microbiol.* **8,** 435–441.
17. Swanson, R. V., Schuster, S. C. & Simon, M. I. (1993) *Biochemistry* **32,** 7623–7629.
18. Surette, M. G., Levit, M., Liu, Y., Lukat, G., Ninfa, E. G., Ninfa, A. & Stock, J. B. (1996) *J. Biol. Chem.* **271,** 939–945.
19. Forst, S., Comeau, D., Norioka, S. & Inouye, M. (1987) *J. Biol. Chem.* **262,** 16433–16438.
20. Roberts, D. L., Bennett, D. W. & Forst, S. A. (1994) *J. Biol. Chem.* **269,** 8728–8733.
21. Aiba, H., Mizuno, T. & Mizushima, S. (1989) *J. Biol. Chem.* **64,** 8563–8567.
22. Delgado, J., Forst, S., Harlocker, S. & Inouye, M. (1993) *Mol. Microbiol.* **10,** 1037–1047.
23. Igo, M. M., Ninfa, A. J., Stock, J. B. & Silhavy, T. J. (1989) *Genes Dev.* **3,** 1725–1734.
24. Tokishita, S., Yamada, H., Aiba, H. & Mizuno, T. (1990) *J. Biochem.* **108,** 488–493.
25. Park, H. & Inouye, M. (1997) *J. Bacteriol.* **179,** 4382–4390.
26. Hidaka, Y., Park, H. & Inouye, M. (1997) *FEBS Lett.* **400,** 238–242.
27. Sambrook, J., Fritsch, E. F. & Maniatis, T. (1989) *Molecular Cloning: A Laboratory Manual* (Cold Spring Harbor Lab. Press, Plainview, NY), 2nd Ed., pp 18.56–18.57.
28. Gill, S. C. & VonHippel, P. H. (1989) *Anal. Biochem.* **182,** 319–326.
29. Utsumi, R., Brisette, R. W., Rampersaud, A., Forst, S. A., Oosawa, K. & Inouye, M. (1989) *Science* **245,** 1246–1249.
30. Baumgartner, J. W., Kim, C., Brissette, R. E., Inouye, M., Park, C. & Hazelbauer, G. (1994) *J. Bacteriol.* **176,** 1157–1163.